intermediate. Because of the polarization by the Zn(II), this intermediate is activated toward hydrolysis through polarization of the carbonyl bonds by the active-site Zn(II). Such an interaction would result in a decrease in electron density about the carbonyl carbons, thereby making them more susceptible to nucleophilic attack. While each carbonyl is activated toward attack, it is possible that the enzyme has evolved to hydrolyze preferentially at only one of the sites. Work by Nau and Riordan suggests this may actually be the case.[8] The remainder of the mechanism involves the hydrolysis of the activated intermediate to liberate the acid product.

Registry No. CPA, 11075-17-5; BPLDAB, 140176-20-1; DA, 619-84-1; DAA, 140176-21-2; DAB-Cl, 4755-50-4.

Synthesis and Structure Elucidation of a New [2]-Catenane

Christopher A. Hunter†

Contribution from the Department of Chemistry, University of Otago, P.O. Box 56, Dunedin, New Zealand. *Received August 23, 1991*

Abstract: A supramolecular self-assembly process has lead to the synthesis of new type of [2]-catenane. A 34% yield of catenane was obtained from a one-pot double macrocyclization reaction. Its three-dimensional structure was determined by using two-dimensional ^{1}H NMR spectroscopy. This structure agrees well with the predictions of molecular mechanics calculations, although there is some ambiguity in the orientation of one of the amide bonds. The molecule is locked into a well-defined conformation by several intermacrocycle H-bonds and π–π interactions and it is these interactions that template the assembly of the interlocked ring system. The dynamic properties of the catenane were investigated by variable-temperature ^{1}H NMR. The "inside" and "outside" parts of the molecule do not exchange with one another because of bulky cyclohexyl groups, which act as "spokes" preventing free rotation of the macrocycles. However, the system does possess some conformational mobility, which can be followed on the ^{1}H NMR time scale. A chiral NMR shift reagent was used to show that the [2]-catenane adopts a chiral ground state. It switches between two enantiomeric conformations at a rate of 1 s^{-1} at room temperature.

Introduction

Supramolecular chemistry has revolutionized approaches to the synthesis of topologically complex molecules.[1] Early catenane syntheses relied purely on chance to thread the macrocyclic link.[2] The first efficient catenane synthesis was developed by Schill and Lutteringhaus who used covalent bonds to direct formation of the interlocked ring system.[3] More recently, Sauvage's introduction of the metal ion template has afforded an impressive array of catenanes and molecular knots.[4] In nature, weaker intermolecular forces such as H-bonding and π–π interactions are used to template the extremely efficient syntheses that characterize biological self-assembly and self-replication.[5] Stoddart has demonstrated the power of this approach with his supramolecular catenane and rotaxane syntheses.[1,6] In these remarkable systems, π–π interactions provide the major driving force for self-assembly: they direct and template threading of the macrocyclic links.

In this paper, I report the synthesis and NMR structure determination of a new class of [2]-catenane. The molecule is locked into a well-defined conformation by a combination of H-bonds and π–π interactions and it is these interactions that template the formation of the interlocked ring system. A supramolecular self-assembly process results in a 34% yield of [2]-catenane in a one-pot double-macrocyclization reaction.

Results and Discussion

Synthesis. I recently reported the synthesis of **1**, a receptor for *p*-benzoquinone.[7] This synthesis employed the macrocyclization reaction shown in Scheme I. In an attempt to improve the yield of **1**, I developed the two-step synthesis shown in Scheme II. This reaction yielded three major products, fractions A, B, and C (see Experimental Section). Fraction B was identical with the cyclic dimer, **1**, synthesized via Scheme I. FAB mass spectra of fractions A and C showed molecular ions that corresponded to tetrameric species. Fraction C had a ^{1}H NMR spectrum that was almost identical with that of **1** in $CDCl_3/CD_3OD$. Thus all four components of the tetramer were equivalent and had retained their symmetry. In contrast, fraction A had a very complex ^{1}H NMR spectrum (see below). There were several sets of nonequivalent protons and some signals showed large changes in chemical shift

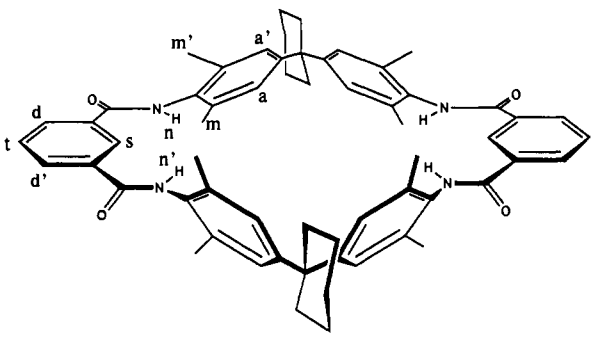

1

† Current address: Department of Chemistry, The University, Sheffield S3 7HF, United Kingdom.

(1) (a) Ashton, P. R.; Goodnow, T. T.; Kaifer, A. E.; Reddington, M. V.; Slawin, M. Z.; Spencer, N.; Stoddart, J. F.; Vincent, C.; Williams, D. J. *Angew. Chem., Int. Ed. Engl.* **1989**, *28*, 1396–1399. (b) Ashton, P. R.; Brown, C. L.; Chrystal, E. J. T.; Goodnow, T. T.; Kaifer, A. E.; Parry, K. P.; Philp, D.; Slawin, M. Z.; Spencer, N.; Stoddart, J. F.; Williams, D. J. *J. Chem. Soc., Chem. Commun.* **1991**, 634–639. (c) Stoddart, J. F. *Chem. Br.* **1991**, 714–718 and references cited therein.

(2) Wasserman, E. *J. Am. Chem. Soc.* **1960**, *82*, 4433–4434.

(3) (a) Schill, G. *Catenanes, Rotaxanes and Knots*; Academic Press: New York, 1971. (b) Walba, D. M. *Tetrahedron* **1985**, *41*, 3161–3212 and references cited therein.

(4) (a) Dietrich-Buchecker, C. O.; Sauvage J.-P. *Tetrahedron Lett.* **1983**, *24*, 5095–5098. (b) Sauvage, J.-P. *Chem. Rev.* **1987**, *87*, 795–810. (c) Mitchell, D. K.; Sauvage, J.-P. *Angew. Chem., Int. Ed. Engl.* **1988**, *27*, 930–931. (d) Dietrich-Buchecker, C. O.; Sauvage, J.-P. *Angew. Chem.* **1989**, *28*, 189–192. (e) Sauvage, J.-P. *Acc. Chem. Res.* **1990**, 319–327 and references cited therein.

(5) (a) Naylor, R.; Gilham, P. T. *Biochemistry* **1966**, *5*, 2723–2728. (b) Orgel, L. E.; Lohrmann, R. *Acc. Chem. Res.* **1974**, *7*, 368–377. (c) von Kiedrowski, G. *Angew. Chem., Int. Ed. Engl.* **1986**, *25*, 932–935. (d) Zielinski, W. S.; Orgel, L. E. *Nature* **1987**, *327*, 346–347. For some applications of these principles to the synthesis of "unnatural" catenated and knotted DNA's, see: (e) Chen, J.; Seeman, N. C. *Nature* **1991**, *350*, 631–633. (f) Mueller, J. E.; Du, S. M.; Seeman, N. C. *J. Am. Chem. Soc.* **1991**, *113*, 6306–6308.

0002-7863/92/1514-5303$03.00/0

compared with the signals observed for **1**. These shifts and the unusually high R_f observed for this fraction implied the presence of intramolecular H-bonding and π–π interactions: some of the polar amide groups were buried inside the molecule and could not interact with the solvent.

Two isomeric tetramer structures are possible: the cyclic tetramer, **2**, and the [2]-catenane, **3**, which is comprised of two interlocked cyclic dimers. The evidence presented above implies

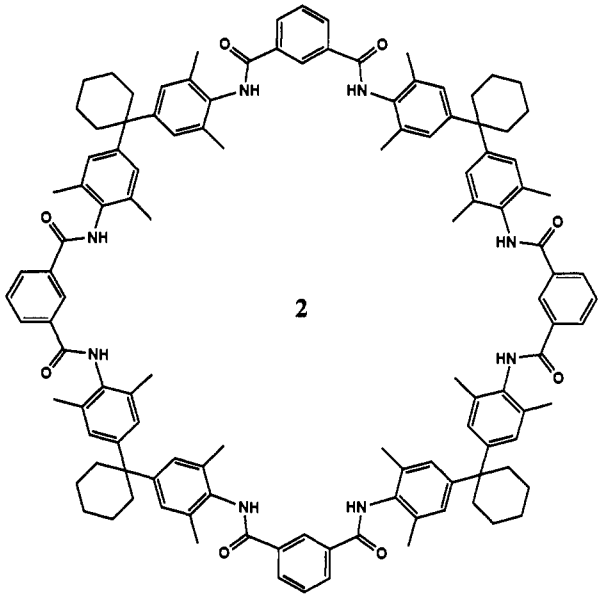

2

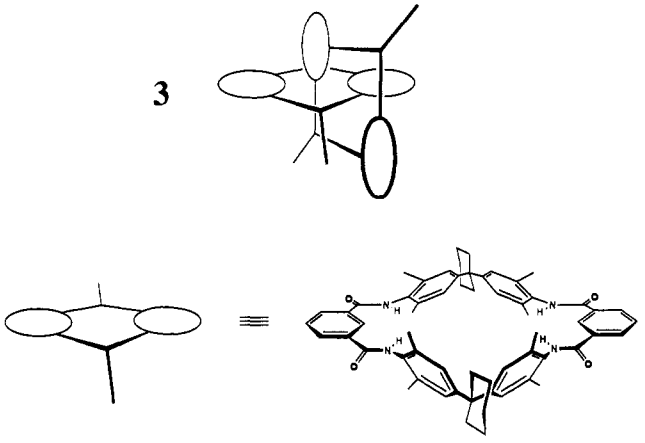

3

that fraction A has the catenane structure, **3**, while fraction C is the cyclic tetramer, **2**. The fragmentation patterns observed in the FAB mass spectra also support this conclusion. Fraction A showed no fragment ions between 1806 (tetramer) and 905 (dimer), whereas fraction C had several fragment ions in this region.[1a,8] However, in order to rule out the possibility that fraction A is a twisted or knotted form of the cyclic tetramer, I have carried out a detailed ^{1}H NMR study to determine the three-dimensional structure of this molecule in solution.

Three-Dimensional Structure Determination. The ^{1}H NMR spectrum of fraction A varied with solvent and temperature. Several exchange processes were occurring on the chemical shift time scale. In $CDCl_3$, the resonances were broadened due to aggregation and, surprisingly, the compound was only sparingly soluble in CD_2Cl_2. It was very soluble in $C_2D_2Cl_4$ and a sharp well-resolved spectrum was obtained in this solvent. However, the resonances broadened on cooling and the slow-exchange limit could not be reached without aggregation. Addition of traces of methanol-d_4 increased the solubility in all three solvents and inhibited aggregation so that sharp well-resolved spectra were obtained. The chemical shifts of some of the amide signals were altered due to H-bonding to the methanol-d_4 but the rest of the spectrum was essentially unchanged, indicating that no gross conformational changes had occurred. A sharp well-resolved slow-exchange spectrum was obtained in CD_2Cl_2/CD_3OD at −50 °C and these conditions were used for the structure determination described below.

In the following discussion, the protons are labeled according to the scheme shown in structure **1**. Numerical subscripts are used to differentiate nonequivalent aromatic rings. Dashes are used to differentiate nonequivalent sides of the same aromatic ring. The NH protons are numbered and dashed according to the isophthaloyl group to which they are attached. Numbering of the *m*-xylyl groups is arbitrary. The cyclohexyl signals were broad and poorly resolved and contained little structural information.

The amide signals (n) were assigned by exchange with deuterium (Figure 1). Two of the amide protons exchanged slowly,

Scheme I

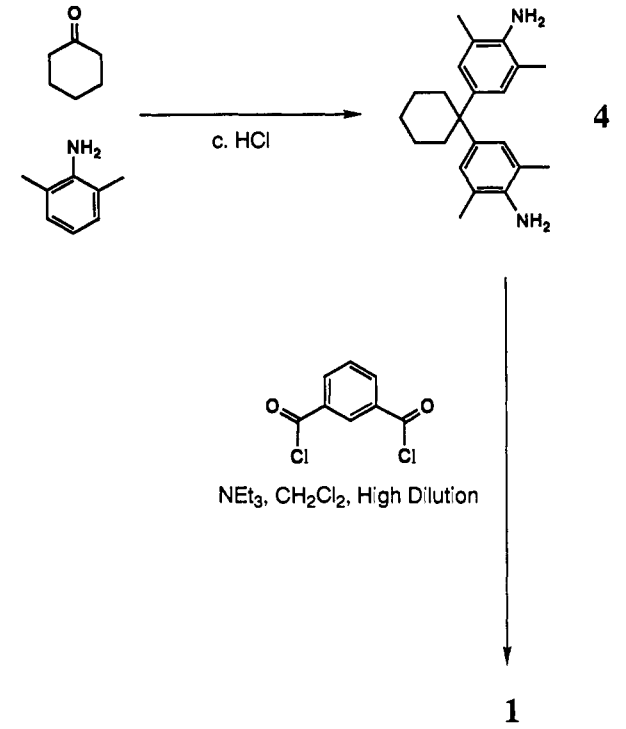

Scheme II

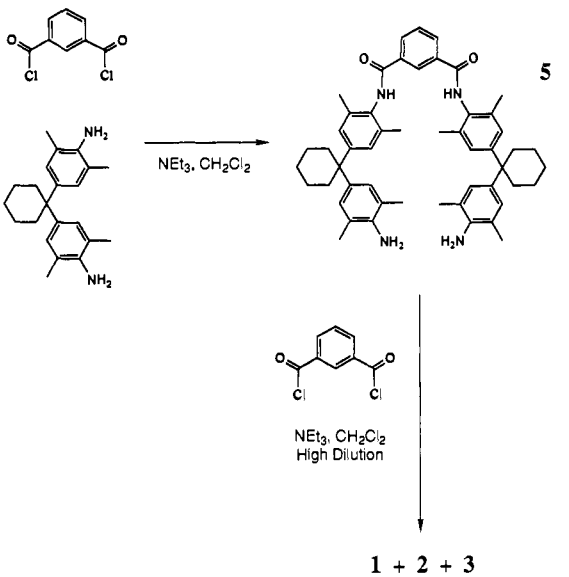

(6) See also Tjlvikua, T.; Ballester, P.; Rebek, J., Jr. *J. Am. Chem. Soc.* **1990**, *112*, 1249–1250.
(7) Hunter, C. A. *J. Chem. Soc., Chem. Commun.* **1991**, 749–751.
(8) (a) Vetter, W.; Logeman, E.; Schill, G. *Org. Mass Spectrom.* **1977**, *12*, 351–369. (b) Dietrich-Buchecker, C. O.; Sauvage, J.-P. *J. Am. Chem. Soc.* **1984**, *106*, 3043–3045.

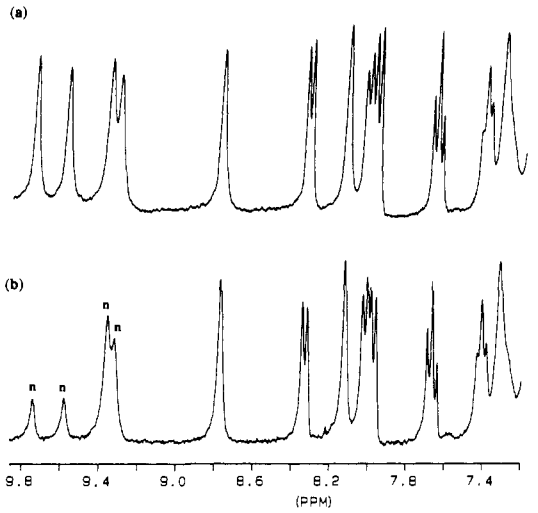

Figure 1. Isophthaloyl region of the 300-MHz ^{1}H NMR spectra of fraction A in CD_2Cl_2/CD_3OD at −50 °C. (a) Spectrum recorded immediately on addition of CD_3OD. (b) Spectrum recorded after incubation at 0 °C for 8 days. The amide signals that exchanged with deuterium are marked n.

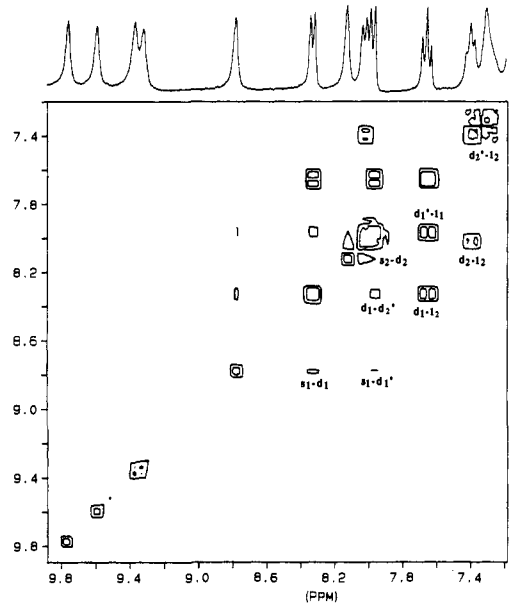

Figure 2. Isophthaloyl region of the 300-MHz COSY spectrum of fraction A in CD_2Cl_2/CD_3OD at −50 °C.

while two exchanged rapidly. The two high-field amide signals that exchanged slowly are due to protons that are buried inside the molecule and are involved in intramolecular H-bonds. In contrast, the two low-field amide signals are due to protons that are exposed to solvent and so exchange more rapidly with deuterium.[9]

The spin systems were assigned by using a COSY experiment. This revealed the presence of two nonequivalent isophthaloyl moieties (Figure 2). Long-range coupling observed between the d and d′ protons indicates that the 2-fold symmetry of the isophthaloyl groups has also been destroyed: the two sides of each ring are nonequivalent.[10] The assignment of the four amide signals was confirmed by the lack of cross-peaks to these signals.

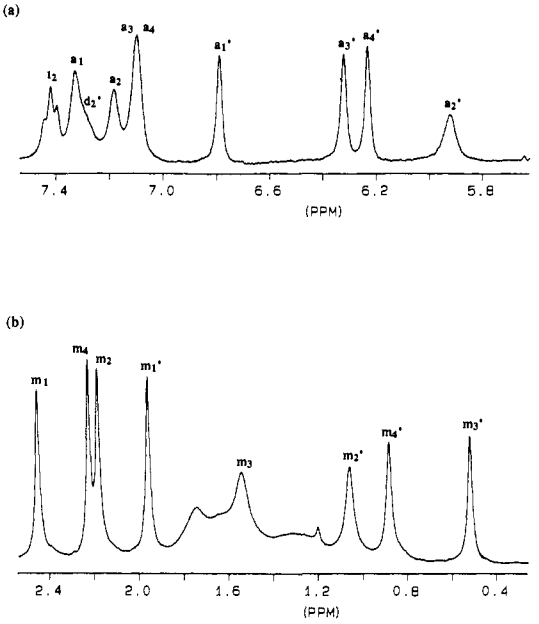

Figure 3. Sections of the 300-MHz ^{1}H NMR spectrum of fraction A in CD_2Cl_2/CD_3OD at −50 °C: (a) the a region; (b) the methyl region.

Cross-peaks were also observed among the a signals. There were eight nonequivalent signals in this region of the spectrum but meta-coupling cross-peaks revealed the presence of only four nonequivalent *m*-xylyl fragments (Figure 3). No cross-peak was observed between a_2 and a_2', but these signals were assigned by a process of elimination.[10] This assignment was confirmed by variable-temperature experiments, which showed that a_2 and a_2' exchange with one another and at a similar rate to the related $m_2 \leftrightarrow m_2'$ exchange process (see later). Long-range coupling between the a and m signals allowed partial assignment of the methyl region of the spectrum (Figure 3b). m_1, m_1', m_3', m_4, and m_4' were assigned on the basis of COSY cross-peaks. Expected a–m cross-peaks, which were missing in this region of the spectrum, all involved broadened signals.[10] The remaining unassigned methyl signals, m_2, m_2', and m_3, were assigned by using the NOESY experiments described below. Remarkably, there were only two overlapping sets of signals in the spectrum: d_2' and a_1 were coincident as were a_3 and a_4.

The COSY results indicate that the molecule has 2-fold symmetry: there are a total of four isophthaloyl fragments, which are present as two nonequivalent pairs; there are a total of eight *m*-xylyl fragments, which are present as four nonequivalent pairs; there are a total of eight amide protons, which are present as four nonequivalent pairs. These fragments were pieced together by using NOESY experiments.

NOESY spectra were initially acquired at room temperature, but they showed very little NOE information and were dominated by negative chemical exchange cross-peaks. However, when the experiments were repeated at −50 °C, very few exchange cross-peaks were observed and the spectra were dominated by negative NOE cross-peaks. The measured T_1 values increased by a factor of 2 on cooling, reflecting the decrease in the rate of molecular tumbling. This was sufficient to move the system from the zero-tumbling regime at 25 °C to the negative NOE regime at −50 °C. In contrast, the rates of chemical exchange decreased by several orders of magnitude on cooling (see variable-temperature experiments later). Thus the chemical exchange processes were fast on the T_1 time scale at 25 °C but slow at −50 °C and the switch from a chemical exchange dominated spectrum at 25 °C to an NOE dominated spectrum at −50 °C was very efficient.

NOESY experiments were carried out at −50 °C using mixing times of 0.4 and 1.0 s. The following discussion concentrates on cross-peaks observed in both experiments. Additional cross-peaks, which were only observed for the longer mixing time, were attributed to long-range NOEs. Figure 4 shows relevant sections of the NOESY spectrum acquired with a 1.0-s mixing time.

(9) The chemical shifts of the amide signals imply that they are all involved in H-bonding. However, some of these interactions are likely to be with the methanol solvent.

(10) The data were processed by using a resolution-enhancement apodization function so that cross-peaks due to the broad signals were reduced in intensity. Thus long-range coupling between d_2 and d_2', although apparent in traces, was low in the noise and does not show up in Figure 4. Similarly, cross-peaks involving long-range coupling to a_2, a_2', and m_3 were not observed.

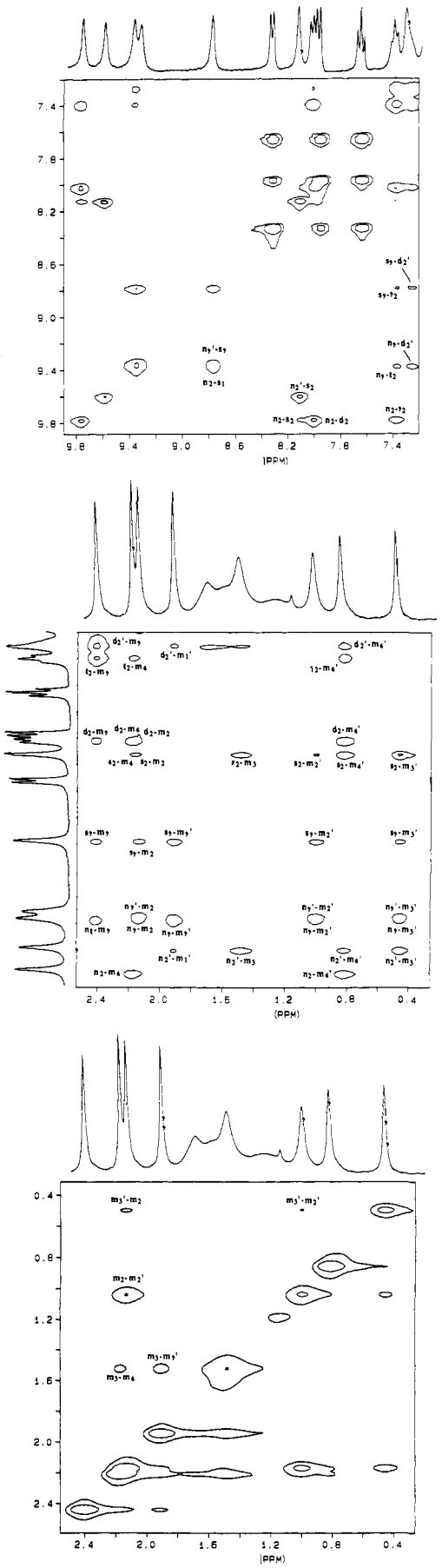

Figure 4. Sections of the 300-MHz NOESY spectrum of fraction A in CD_2Cl_2/CD_3OD at −50 °C: (a, top) the isophthaloyl region (cross-peaks that are not labeled were also observed in the COSY spectrum); (b, middle) the isophthaloyl–methyl region; (c, bottom) the methyl region.

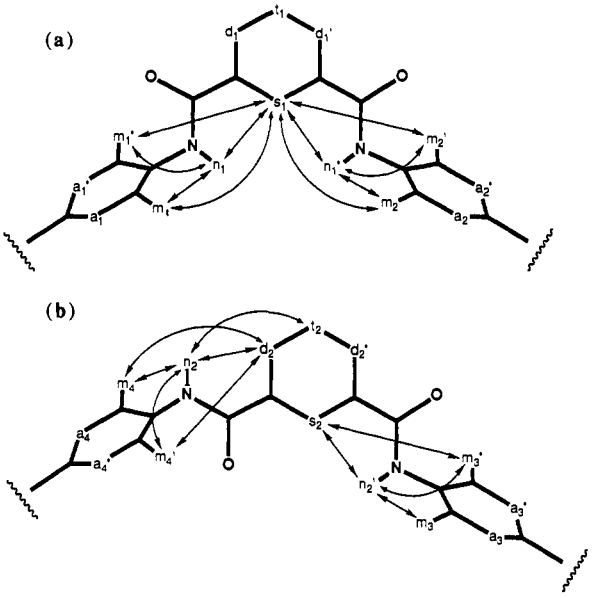

Figure 5. NOEs that establish covalent connectivity. Multiple bonds and carbon atoms have been omitted for clarity. n_1 also gave weak NOEs to m_2 and m_2'.

Figure 4a is the isophthaloyl region of the spectrum. Cross-peaks that are not labeled are simply signals that were also observed in the COSY spectrum and do not contain any additional structural information. This region of the spectrum allows connection of the amide protons to the appropriate isophthaloyl groups and definition of the stereochemistries of these fragments (Figure 5).[11] One isophthaloyl moiety (labeled 1) has two convergent NH groups. In contrast, the n_2–d_2 and n_2–t_2 cross-peaks indicate that n_2 in isophthaloyl 2 is "flipped out" (Figures 5b). The weak NOE between n_2 and s_2 in Figure 4a was not observed in the 0.4-s mixing time experiment and was assigned as a long-range interaction, consistent with the stereochemistry in Figure 5b.

m–n NOEs in Figure 4b connect the *m*-xylyl fragments to the appropriate the isophthaloyl moieties (Figure 5) and enable assignment of the methyl signals, m_2, m_2', and m_3, which were not assigned by the COSY experiment.

The other NOEs in Figure 4a,b indicate that the two fragments shown in Figure 5 are closely associated. The rate of exchange of the amide protons with deuterium imply that it is H-bonding interactions involving n_1 and n_1' that are responsible for this association (Figure 6a). Isophthaloyl 2 is bound in the cavity created by isophthaloyl 1, *m*-xylyl 1, and *m*-xylyl 2. NOEs from n_1, n_1', and s_1 to m_3' indicate that *m*-xylyl 3 is also bound in this cleft and cross-peaks in the methyl region of the NOESY spectra confirm this (Figures 4c and 6b). The information in Figure 6 can be translated into a three-dimensional representation of this part of the molecule (Figure 7). This structure represents the asymmetric unit of fraction A and the complete molecule is comprised of two of these units.

The m_3–m_4 cross-peak suggests that m_3 is wedged in a diarylmethane cleft formed by *m*-xylyl 1 and *m*-xylyl 4. NOEs between m_4' and s_2, d_2', and t_2 imply that *m*-xylyl 4 lies over the face of isophthaloyl 2. These observations are consistent with a covalent connection between *m*-xylyl 1 and *m*-xylyl 4. Until now no use has been made of NOEs observed for the a signals. There are a large number of cross-peaks involving these signals and their interpretation is hampered by the fact that a_1 overlaps with d_2' and a_4 overlaps with a_3. However, the NOE pattern in this region of the spectra confirms that the *m*-xylyl fragments are indeed connected in a 1–4 and 2–3 manner. A full set of NOEs was observed between the a signals and the signals due to their neighboring ortho methyl groups. A self-consistent interpretation

(11) It was assumed that the amide bonds adopt trans conformations and this is supported by the molecular modeling results.

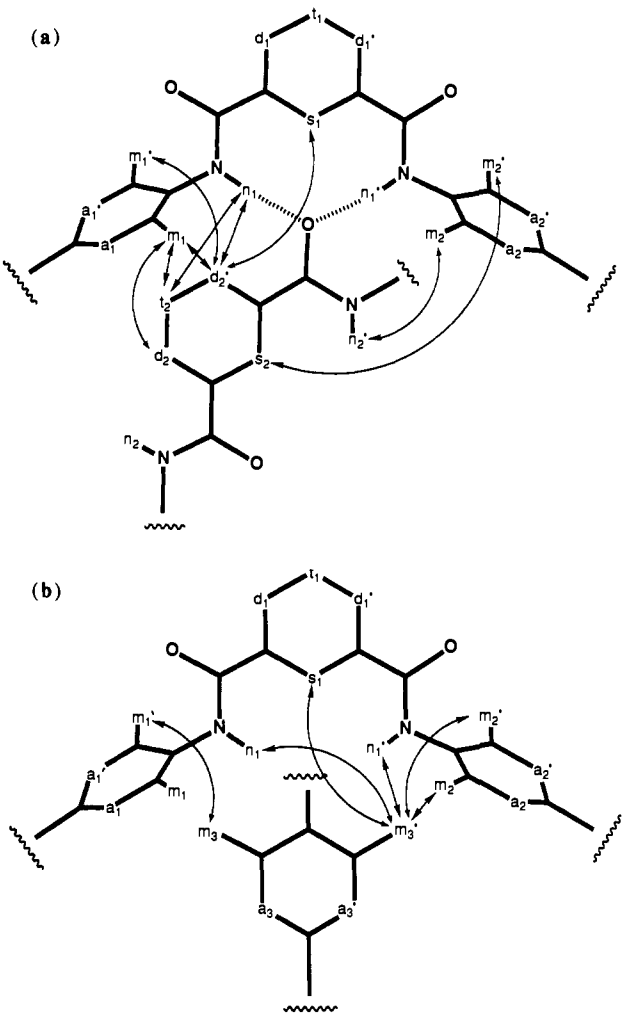

Figure 6. NOEs that establish noncovalent connectivity. Multiple bonds and carbon atoms have been omitted for clarity.

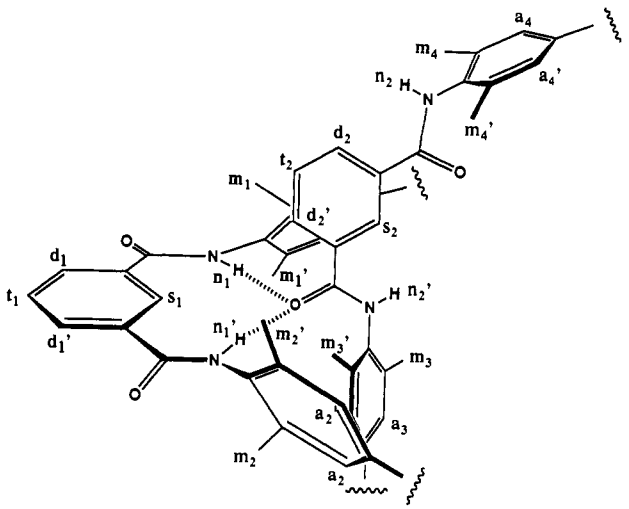

Figure 7. NMR-derived three-dimensional structure of the asymmetric unit of fraction A.

of the remaining NOEs is illustrated in Figure 8. The only NOE that is missing from this pattern is between a_2' and m_3, the two broadest signals in the spectrum. Alternative modes of *m*-xylyl connectivity do not yield a similar correlation with the NOE data.

The only other cross-peaks that have not yet been accounted for are a_2–a_2', m_2–m_2', and m_3–a_1'. The m_3–a_1' NOE might be interpreted as evidence of a 1–3 *m*-xylyl connectivity pattern. However, the corresponding a_1–a_3', m_1–a_3', and m_3'–a_1 NOEs were not observed so this possibility can be excluded. The m_3–a_1'

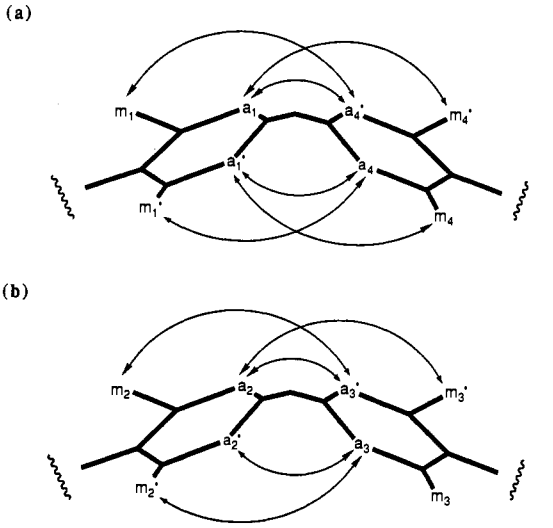

Figure 8. NOEs that establish the *m*-xylyl covalent connectivity pattern in the diarylmethane units.

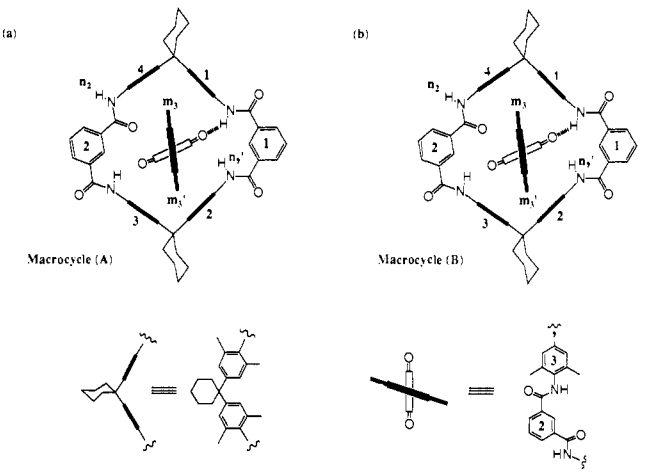

Figure 9. Schematic representation of the NMR-derived structure of fraction A. The structure was energy minimized by using the CHARMm force-field.[12] H-bonds are shown as dashed lines. (a) Macrocycle A with the isophthaloyl 2 and *m*-xylyl 3 of macrocycle B bound inside its cavity. (b) Macrocycle B with the isophthaloyl 2 and *m*-xylyl 3 of macrocycle A bound inside its cavity.

cross-peak is consistent with the three-dimensional structure shown in Figure 7 and is related to the m_3–m_1' NOE in Figure 6b. The a_2–a_2' and m_2–m_2' cross-peaks are due to fast rotation of *m*-xylyl 2 about its axis on the T_1 time scale. The measured activation energy for this process confirms this assignment (see variable-temperature experiments later).

The 1–4 and 2–3 *m*-xylyl connections yield the [2]catenane structure **3**. The final structure, which is illustrated schematically in Figure 9, was energy minimized by using the CHARMm force-field.[12] Each macrocycle may be considered as a square box. The *m*-xylyl 3 units fit diagonally across the box, while the isophthaloyl 2 groups are aligned almost parallel to two of the box sides. Molecular mechanics indicated the presence only two H–bonds, between the n_1 protons and the n_2' carbonyl oxygens (Figure 9). The n_1' protons are very close to the n_2' carbonyl oxygens but lie just outside the CHARMm H-bonding cut-off distance. Model-building studies using CPK models and molecular mechanics showed that it is impossible to construct a twisted conformation of the cyclic tetramer, which is consistent with the NMR data. In contrast, two cyclic dimers fit together almost perfectly: there is essentially no bond strain and no empty space inside the macrocyclic cavities.

(12) Brooks, B. R.; Bruccoleri, R. E.; Olafson, B. D.; States, D. J.; Swaminathan, S.; Karplus, M. *J. Comput. Chem.* **1983**, *4*, 187.

Table I. Change in ^{1}H NMR Chemical Shifts of **3** Relative to **1** ($\Delta\delta$ in ppm)

proton	$\Delta\delta^a$	$\Delta\delta^b$	proton	$\Delta\delta^a$	$\Delta\delta^b$
n_1		+1.65	n_2		+0.10
n_1'		+1.65	n_2'		+0.59
s_1	+0.56	+0.89	s_2	−0.10	−0.10
d_1	+0.28	+0.22	d_2	−0.03	−0.41
d_1'	−0.08	+0.10	d_2'	−0.74	−0.56
t_1	+0.09	0.00	t_2	−0.16	−0.22
a_1	+0.26	+0.26	a_3	+0.18	+0.12
a_1'	−0.13	−0.26	a_3'	−0.59	−0.71
a_2	+0.41	+0.12	a_4	+0.18	−0.01
a_2'	−0.99	−1.08	a_4'	−0.68	−0.71
m_1	+0.37	+0.32	m_3	−0.55	−0.79
m_1'	−0.13	−0.23	m_3'	−1.57	−1.61
m_2	+0.10	−0.03	m_4	+0.14	+0.07
m_2'	−1.03	−1.18	m_4'	−1.21	−1.29

^{a}Solvent CD_2Cl_2/CD_3OD. Chemical shifts for **1** are H_s = 8.23; H_d = 8.06; H_t = 7.57; H_a = 6.91; H_m = 2.09. ^{b}Solvent $C_2D_2Cl_4$. Chemical shifts for **1** are H_s = 8.19; H_d = 8.16; H_t = 7.69; H_a = 7.04; H_m = 2.18.

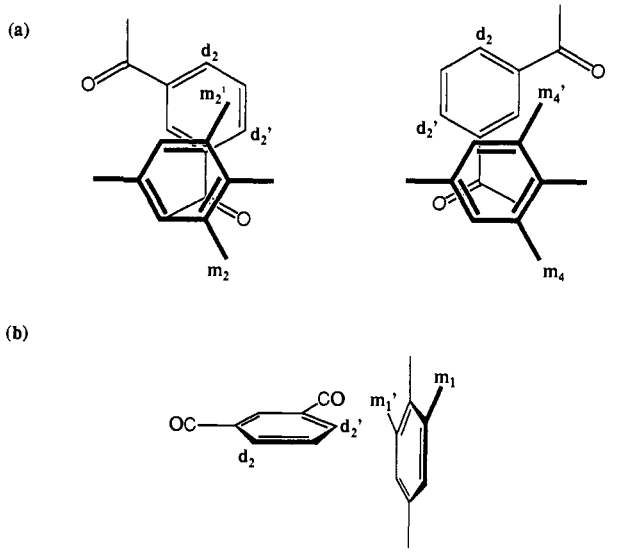

Figure 10. Intermacrocycle $\pi-\pi$ interactions in the [2]-catenane. (a) Offset π-stacking interactions sandwich isophthaloyl 2 of one macrocycle between *m*-xylyl 2 and *m*-xylyl 4 of the other. (b) Edge-to-face $\pi-\pi$ interactions between isophthaloyl 2 of one macrocycle and *m*-xylyl 1 of the other.

The changes in chemical shift of the catenane signals relative to those observed for the cyclic dimer, **1**, are listed in Table I and may be intepreted with reference to the intermacrocycle interactions shown in Figures 7, 9, and 10. The signals that experience large shifts are all due to protons in the interior of the molecule as might be expected. The shift observed for s_1 is due to the deshielding effect of the H-bonded carbonyl group of isophthaloyl 2 and is similar to the shift observed when **1** binds *p*-benzoquinone.[7] d_2' lies inside the macrocyclic cavity, over the faces of *m*-xylyl 1, *m*-xylyl 2, and *m*-xylyl 4 and so experiences a large upfield ring-current-induced shift (Figure 10). The upfield shifts on a_2' and m_2' indicate that this side of *m*-xylyl 2 lies over the face of isophthaloyl 2 (Figure 10a). Similarly, the upfield shifts on a_4' and m_4' indicate that this side of *m*-xylyl 4 lies over the other face of isophthaloyl 2 (Figure 10a). The large upfield shifts observed for a_3' and m_3' show that this side of *m*-xylyl 3 is embedded deep in the diarylmethane cleft between *m*-xylyl 2 and the other *m*-xylyl 3 (Figure 9). m_3 also experiences an upfield shift placing it in the diarylmethane cleft between *m*-xylyl 1 and *m*-xylyl 4 (Figure 9). In contrast, a_3 is not shifted. a_3 experiences a compensating downfield shift because it lies in the deshielding zone of the n_2 carbonyl oxygen, which is directed toward the center of the macrocyclic cavity (Figure 9). a_1 and m_1 experience downfield shifts indicative of an edge-to-face $\pi-\pi$ interaction with isophthaloyl 2 (Figure 10b). Thus isophthaloyl 2 is involved in offset π-stacking interactions with *m*-xylyl 2 and *m*-xylyl 4 and an edge-to-face $\pi-\pi$ interaction with the face of *m*-xylyl 1 (Figure 10).[13]

Table II. ^{1}H NMR Relaxation Times for **3** (T_1 in s)^a

proton	T_1	proton	T_1
n_1	0.79	n_2	1.00
n_1'	0.86	n_2'	0.93
s_1	0.81	s_2	1.09
d_1	2.11	d_2	1.13
d_1'	1.95	d_2'	
t_1	1.94	t_2	1.18
a_1	0.77	a_3	0.69
a_1'	0.75	a_3'	0.71
a_2	0.73	a_4	0.69
a_2'	0.78	a_4'	0.82
m_1	1.02	m_3	0.76
m_1'	0.91	m_3'	0.84
m_2	1.02	m_4	1.01
m_2'	0.91	m_4'	1.10

^{a}Solvent CD_2Cl_2/CD_3OD; temperature = −50 °C.

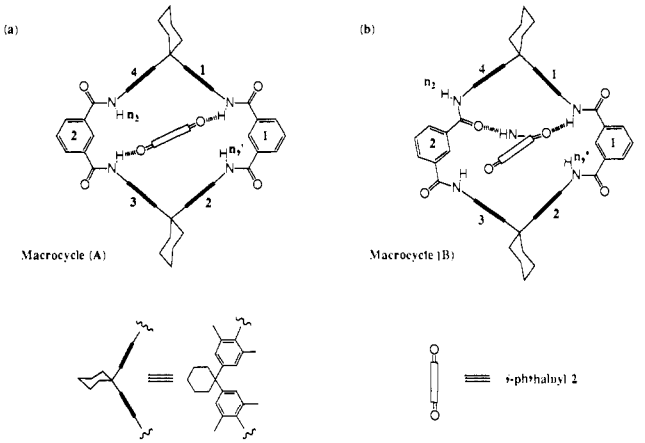

Figure 11. Schematic representation of the molecular mechanics-derived structure of the [2]-catenane. The structure was determined by using an annealed molecular dynamics simulation and the CHARMm force-field.[12] H-bonds are shown as dashed lines. (a) Macrocycle A with the isophthaloyl 2 of macrocycle B bound inside its cavity. (b) Macrocycle B with the isophthaloyl 2 of macrocycle A bound inside its cavity.

The measured T_1 values are also consistent with the [2]-catenane structure (Table II). Protons in the interior of the molecule are close to several methyl groups and relax very rapidly, while those on the outside relax slowly. For example, t_2 that is inside one of the macrocyclic rings relaxes twice as quickly as t_1 that is on the periphery of the molecule.

Molecular Modeling. The catenane structure was investigated by using molecular modeling and the CHARMm force-field.[12] The minimum-energy conformation was determined by using an annealed molecular dynamics simulation and the result is illustrated schematically in Figure 11. The structures in Figures 9 and 11 differ in only one respect, the conformation of the n_2 amide groups. The NMR structure has both n_2 amide protons directed out of the macrocyclic cavity, while the molecular mechanics structure has only one of these amide protons directed outward (compare the conformations of the macrocycle (A) in Figures 9a and 11a).

There are two H-bonds in the NMR-derived conformation and three in the molecular mechanics-derived conformation. In both cases, there is only one H-bond between the amide protons of isophthaloyl 1 and the carbonyl oxygen of isophthaloyl 2. This H-bond involves n_1. The second amide proton, n_1', is significantly further away from the oxygen atom. The third H-bond predicted

(13) (a) Hunter, C. A.; Sanders, J. K. M. *J. Am. Chem. Soc.* **1990**, *112*, 5525–5534 and references cited therein. (b) Severance, D. L.; Jorgensen, W. L. *J. Am. Chem. Soc.* **1990**, *112*, 4768–4774.

Table III. Molecular Mechanics Calculations[a]

compd	CHARMm energy, kJ mol^{-1}
1	330
2	559
3	375

[a] Minimum energy conformations were calculated by using annealed molecular dynamics simulations. Solvent not included.

by the molecular mechanics calculation is between the two isophthaloyl 2 groups across the center of the catenane. One of the n_2' protons is H-bonded to one of the n_2 carbonyl oxygens on the opposite isophthaloyl group. The NMR-derived conformation (Figure 9) was 53 kJ mol^{-1} higher in energy than the molecular mechanics energy minimum. A third conformer, which is similar to the NMR-derived structure but with both n_2' protons H-bonded to both n_2 carbonyl oxygens, was 77 kJ mol^{-1} higher in energy than the minimum.

There are two possible reasons for the discrepancy between the NMR and molecular mechanics structures. Solvent was not used in the molecular mechanics calculations and H-bonding interactions with the methanol-d_4 used in the NMR experiments may stabilize the conformation in Figure 9 over that in Figure 11. In addition, limitations in the way the CHARMm force-field treats $\pi-\pi$ interactions probably contribute to the different results.[13] However, the weak n_2-s_2 NOE in Figure 6a could be interpreted as evidence for the molecular mechanics-derived conformation with fast exchange between the "in" and "out" amide conformations.

Sharp well-resolved spectra were obtained in $C_2D_2Cl_4$ in the absence of methanol-d_4. However, these did not resolve the conformational ambiguity. The spectra were similar to those obtained in CD_2Cl_2/CD_3OD so that most of the resonances could be assigned (Table I). These assignments were confirmed by coalescences observed in variable-temperature experiments (see later). H-bonding to the solvent does not occur in $C_2D_2Cl_4$ so that the chemical shifts of the amide signals are diagnostic of the extent of intramolecular H-bonding. However, since the amide signals shifted significantly on changing the solvent, their assignment by comparison with the CD_2Cl_2/CD_3OD spectrum was not unambiguous. Two of the amide signals were shifted downfield by 1.65 ppm relative to the amide signals in **1**, indicating that they are involved in intramolecular H-bonding. By analogy with the CD_2Cl_2/CD_3OD results, these were assigned as n_1 and n_1'. One of the n_2 signals was not shifted and is not involved in H-bonding. The other n_2 signal experienced a 0.59 ppm downfield shift. This is evidence of the H-bonding interaction involving n_2' but the shift is less than that observed for the other H-bonded protons. There are three possible interpretations: n_2' is in fast exchange between H-bonded and non-H-bonded environments; n_2' is fully H-bonded but is shifted upfield by the ring currents of the cavity side-walls; n_2' is involved in long, relatively weak H-bonds. Thus the three conformational possibilities discussed above cannot be distinguished on the basis of the NMR experiments.

The minimum-energy conformations of the cyclic dimer, **1**, and the cyclic tetramer, **2**, were also computed by using annealed molecular dynamics. Table III lists the calculated energies for these structures. Although the calculations neglected solvent, they show that there is a very large thermodynamic driving force, which favors the formation of catenane over cyclic tetramer.

Chemical Exchange Processes. The dynamic properties of this system were investigated by using variable-temperature ^{1}H NMR. The slow-exchange spectrum in CD_2Cl_2/CD_3OD has already been described in detail. The slow-exchange limit was also reached in $C_2D_2Cl_4$ at −40 °C (300 MHz), albeit with aggregation-induced broadening. The chemical shifts of the signals in this spectrum were identical with those of the CD_2Cl_2/CD_3OD slow-exchange spectrum with the exception of the amide signals, which have been discussed above. The fast-exchange limit was reached at 135 °C (200 MHz) in $C_2D_2Cl_4$ (Figure 12a). The spectrum simplified on heating and there are only two sets of nonequivalent signals in Figure 12a. A detailed variable-temperature experiment revealed several different exchange processes: rotation of the *m*-xylyl

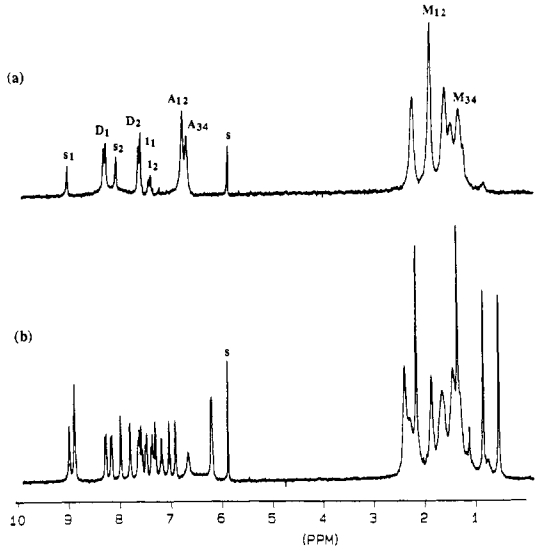

Figure 12. ^{1}H NMR spectra of fraction A in $C_2D_2Cl_4$. (a) 200-MHz spectrum at 135 °C. (b) 300-MHz spectrum at 25 °C. s = solvent. D_1 is the fast-exchange averaged signal of d_1 and d_1'. Similar notation is used for D_2. A_{12} is the fast-exchange averaged signal of a_1, a_1', a_2, and a_2'. Similar notation is used for A_{34}, M_{12}, and M_{34}.

Table IV. Chemical Exchange Processes in **3**[a]

exchange process	$\Delta\delta$, Hz[b]	T_c, K[c]	$\Delta G^{\ddagger}$, kJ mol^{-1} [d]
$\mathbf{a_2} \leftrightarrow \mathbf{a_2'}$	339	283	54
$\mathbf{m_2} \leftrightarrow \mathbf{m_2'}$	380	298	56
$\mathbf{a_1} \leftrightarrow \mathbf{a_1'}$	104	318	64
$\mathbf{m_1} \leftrightarrow \mathbf{m_1'}$	111	338	68
$\mathbf{d_1} \leftrightarrow \mathbf{d_1'}$	22	343	73
$\mathbf{d_2} \leftrightarrow \mathbf{d_2'}$	29	343	73
$\mathbf{a_1/a_1'} \leftrightarrow \mathbf{a_2/a_2'}$	105	368	74
$\mathbf{m_1/m_1'} \leftrightarrow \mathbf{m_2/m_2'}$	134	368	73
$\mathbf{n_1} \leftrightarrow \mathbf{n_1'} \leftrightarrow \mathbf{n_2/n_2'}$	313	378	73
$\mathbf{a_3} \leftrightarrow \mathbf{a_3'} \leftrightarrow \mathbf{a_4} \leftrightarrow \mathbf{a_4'}$	167	378	75
$\mathbf{m_3} \leftrightarrow \mathbf{m_3'} \leftrightarrow \mathbf{m_4} \leftrightarrow \mathbf{m_4'}$	322	378	73

[a] Solvent $C_2D_2Cl_4$. [b] Difference in chemical shift of exchanging signals. [c] Coalescence temperature. Errors are ±10 K. [d] Errors are ±2 kJ mol^{-1}.

groups about their axes (exchange of the dashed and undashed signals); exchange of the two nonequivalent sides of the isophthaloyl groups (exchange of the dashed and undashed signals); exchange of *m*-xylyl 1 with *m*-xylyl 2, exchange of *m*-xylyl 3 with *m*-xylyl 4. Coalescence temperatures for these processes are listed in Table IV. These were not determined with a high degree of precision because there were so many exchanging and closely-spaced signals in the spectrum. The activation energies in Table IV are accurate to within 2 kJ mol^{-1}, which prevents reliable estimation of $\Delta H^{\ddagger}$ and $\Delta S^{\ddagger}$.[14] However, the values of $\Delta G^{\ddagger}$ in Table IV are relatively insensitive to temperature. This implies that $\Delta S^{\ddagger}$ is small for all the exchange processes, which is reasonable for such a highly-ordered, conformationally-restricted system.

The activation energy for rotation of the outside *m*-xylyls, 1 and 2, about their axes is relatively low. In contrast, the inside *m*-xylyls, 3 and 4, do not rotate about their axes independently. Exchange between the dashed and undashed *m*-xylyl 3 and 4 signals only occurs when *m*-xylyl 3 exchanges with *m*-xylyl 4. The two macrocycles fit together so snugly that the inside *m*-xylyls lose their rotational mobility and are locked into fixed orientations.

The other coalescences that were observed all correspond to a single global conformational exchange process. This is illustrated in Figure 13 by using a minimalist representation to show the key structural features of the catenane. The process involves rotation of the isophthloyl 2 groups through the centers of the macrocyclic

(14) Sandström J. *Dynamic NMR Spectroscopy*; Academic Press: London, 1982; pp 77–123.

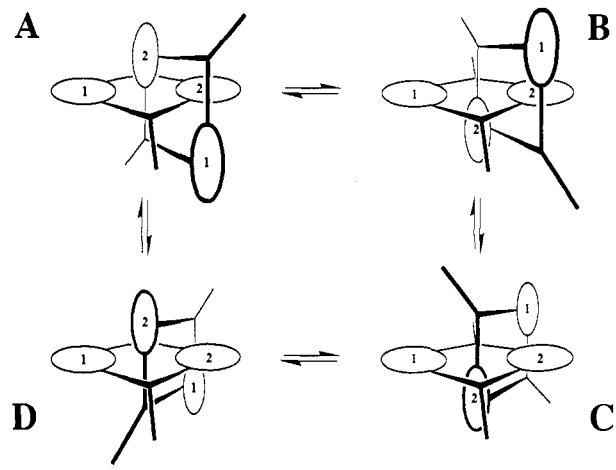

Figure 13. Conformational isomers of **3**. 1 and 2 refer to the labeling system used to distinguish nonequivalent isophthaloyl groups. A and C are different views of the same conformer. B and D are similarly related. However, these two pairs of conformers have different stereochemistries.

Table V. Estimated Rates of Chemical Exchange Processes in **3**

exchange process	rate at 25 °C, Hz	rate at −50 °C, Hz
rotation of *m*-xylyl 2	6×10^2	3×10^{-1}
rotation of *m*-xylyl 1	7×10^0	7×10^{-4}
global conformation exchange	4×10^{-1}	2×10^{-5}

cavities and leads to exchange of the two nonequivalent sides of the isophthaloyl groups as well as exchange of *m*-xylyl 3 with *m*-xylyl 4 and *m*-xylyl 1 with *m*-xylyl 2. The activation energy is large, consistent with the breaking of several H-bonds and π–π interactions associated with this exchange (Table IV).

Exchange of the inside (isophthaloyl 2) and outside (isophthaloyl 1) portions of the molecule was not observed (see Figure 13). This was rationalized by examination of CPK models. The isophthaloyl groups are small enough to rotate through the macrocyclic cavities and this leads to the exchange processes in Figure 13. However, the cyclohexyl groups are too bulky to fit through the macrocyclic cavities and act as spokes, preventing free rotation of the macrocycles about one another. The result is a 90° rocking motion with the inside isophthaloyl groups permanently locked in the interior of the catenane (Figure 13).

If one assumes that the activation energies for the three exchange processes are temperature independent as suggested above, the rates of chemical exchange can be calculated at 25 and −50 °C (Table V). At room temperature, all the exchange processes are fast on the T_1 time scale (≈1 s), but at −50 °C the global conformational exchange process in Figure 13 is slow on the T_1 time scale, as is rotation of *m*-xylyl 1 about its axis. However, rotation of *m*-xylyl 2 about its axis is still fast on the T_1 time scale at −50 °C and correspondingly exchange cross-peaks were observed in the low-temperature NOESY experiment.

Chirality. Conformers A and C in Figure 13 are identical as are conformers B and D, but these two pairs of conformers are different. A/C and B/D are related as nonsuperimposable mirror images and Figure 13 implies that the catenane adopts a chiral ground state. It exists in two enantiomeric forms, which interconvert at a rate of 1 s^{-1} at room temperature.

The chirality of the catenane was investigated by using a chiral NMR shift reagent, Eu((+)-thc)$_3$.[4c,15,16] The catenane was titrated with an single enantiomer of a chiral shift reagent Eu((+)-thc)$_3$ and with an achiral shift reagent, Eu(fod)$_3$. Eu(fod)$_3$ caused larger shifts as it is less sterically crowded and so complexed more strongly with the catenane. Both reagents caused broadening

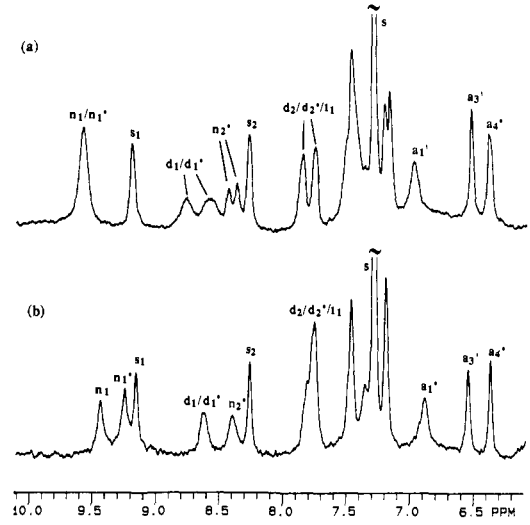

Figure 14. Aromatic region of the ^{1}H NMR spectra of fraction A in $CDCl_3/C_2D_2Cl_4$ in the presence of lanthanide shift reagents: (a) chiral shift reagent, Eu((+)-thc)$_3$; (b) achiral shift reagent, Eu(fod)$_3$; s = solvent.

of the resonances so that some of the signals, such as d_1 and d_1' in Figure 14, were no longer resolved. However, a striking difference in behavior was observed between the two reagents. Figure 14 shows the aromatic region of the ^{1}H NMR spectra at similar stages during the titrations. The chiral reagent caused several signals to split. Two clearly resolved signals were observed for d_1/d_1' and n_2'. a_4' and m_3' also showed small splittings. The appearance of the two spectra in the $t_1/d_2/d_2'$ region also indicates some of these signals are split, although the splitting could not be properly assigned. One apparent anomaly is that n_1 and n_1' appear as one signal in Figure 14a but are resolved in Figure 14b. This is simply an artifact of the different binding properties of the two shift reagents: n_1 and n_1' were resolved at earlier stages in the Eu((+)-thc)$_3$ titration.

Spectral multiplicity due to a chiral shift reagent does not necessarily prove chirality.[16] When an achiral molecule that contains enantiotopic protons binds to a chiral shift reagent, the enantiotopic protons become diastereotopic and splitting can be observed. However, there is no such nonequivalence in the [2]-catenane **3**. For example, although there are two n_2' protons, they are formally equivalent and so the observed splitting must be due to the formation of two diastereomeric complexes. Thus the catenane is present as two enantiomeric species, which are in slow exchange on the chemical shift time scale.

Experimental Section

^{1}H NMR spectra were recorded on Varian VXR 300-MHz and Gemini 200-MHz spectrometers. One-dimensional spectra were typically acquired by using 8K or 16K data points with a spectral width of 12 ppm. COSY and NOESY spectra were acquired by using standard software packages. The phase-sensitive mode was used for the NOESY experiments but not for the COSY. 2K data points were used in f2 and 128 or 256 increments were acquired in f1 with a spectral width of 12 ppm in each dimension. Sixteen to 128 transients were acquired in each increment. Zero-filling was used in f1 but not in f2 and suitable apodization was applied in processing. Lanthanide shift reagent titrations were carried out by recording spectra after successive additions of 1 and 5 mg aliquots of Eu(fod)$_3$ and Eu((+)-thc)$_3$, respectively.

Molecular mechanics calculations were carried out by using a Silicon Graphics Personal Iris 4D-25G and the QUANTA/CHARMm software package.[12] Molecular dynamics simulations were run at 300 K with 0.001-ps time intervals. Typically, heating from 0 to 300 K was carried out over 1 ps, the system was then equilibrated for 4 ps, and the simulation was run for 100 ps. The resulting conformers were then subjected to energy minimization. No solvent was included.

In reactions involving amide bond formation, air and water were rigorously excluded: the apparatus was baked at 500 K for 24 h before use and reagents and solvents were dried.

1,1-Bis(4-amino-3,5-dimethylphenyl)cyclohexane (4). A mixture of 2,6-dimethylaniline (30 mL), cyclohexanone (12.6 mL), and concentrated

(15) Dietrich-Buchecker, C. O.; Edel, A.; Kintzinger, J. P.; Sauvage, J.-P. *Tetrahedron* **1987**, *43*, 333–344.

(16) For a discussion of symmetry and nonequivalence in NMR, see: Sanders, J. K. M.; Hunter, B. K. *Modern NMR Spectroscopy*; Oxford University Press: Oxford, 1987; pp 299–302 and references cited therein.

HCl (30 mL) was refluxed for 48 h. The products were taken up in 500 mL of water, and the solution made basic with 1 M sodium hydroxide and extracted with 1000 mL of chloroform. The solvent was evaporated under reduced pressure and the product crystallized on addition of 500 mL of pentane. The white crystals were filtered off and dried in vacuo, overall yield 20 g (53%). NMR ($CDCl_3$) δ 6.83 (4 H, s), 3.41 (4 H, br s), 2.17 (4 H, br), 2.12 (12 H, s), 1.54 (4 H, br), 1.47 (2 H, br). *m/z* 322 (M^+); $C_{22}H_{30}N_2$ requires M^+ = 322.

Cyclic Dimer 1 (Scheme I). 4, 0.32 g, and 0.27 mL of triethylamine were dissolved in 30 mL of dry dichloromethane and transferred to a dropping funnel. Isophthaloyl dichloride (0.20 g) was similarly dissolved in 30 mL of dry dichloromethane and transferred to an identical dropping funnel. These two solutions were added dropwise to 100 mL of dry dichloromethane over a period of 4 h with stirring under nitrogen. The reaction mixture was then stirred for a further 12 h. The precipitate was filtered off and the solvent evaporated under reduced pressure. The products were chromatographed on silica with chloroform–ethanol (99:1) eluant. The first band eluted was a mixture of several products. These were separated by preparative TLC, eluting with chloroform–ethanol (99:1). The first major band was **1**. It was recrystallized from chloroform–pentane, giving a white powder (44 mg, 10%). NMR ($CDCl_3$/CD_3OD) δ 8.23 (2 H, s), 8.06 (4 H, d), 7.57 (2 H, t), 6.91 (8 H, s), 2.25 (8 H, br), 2.09 (24 H, s), 1.56 (8 H, br), 1.45 (4 H, br). *m/z* 906 (MH^+); $C_{60}H_{64}N_4O_4$ requires M^+ = 904.

Isophthaloyl Bis(diamine) 5. 4, 10 g, was dissolved in 50 mL of dry dichloromethane and 1.4 mL of triethylamine was added. Isophthaloyl dichloride (1 g) was similarly dissolved in 100 mL of dry dichloromethane and transferred to a dropping funnel. The acid chloride was added dropwise to the 4 solution over a period of 2 h with stirring under nitrogen. The reaction mixture was stirred for a further 12 h. The solvent was then evaporated under reduced pressure. The products were chromatographed on silica with chloroform eluant. The first band eluted was **4**. The second major band was the title compound, **5**. It was recrystallized from chloroform–pentane, giving a white powder (2.25 g, 59%). NMR ($CDCl_3$) δ 8.43 (1 H, s), 8.02 (2 H, d), 7.51 (1 H, t), 7.46 (2 H, s), 7.00 (4 H, s), 6.85 (4 H, s), 3.45 (4 H, s), 2.20 (20 H, br m), 2.14 (12 H, s), 1.57 (8 H, br), 1.50 (4 H, br). *m/z* 775 (MH^+); $C_{52}H_{62}N_4O_2$ requires M^+ = 774.

Cyclic Dimer 1, Cyclic Tetramer 2, and Catenane 3 (Scheme II). 5, 1 g, and 0.4 mL of triethylamine were dissolved in 250 mL of dry dichloromethane and transferred to a dropping funnel. Isophthaloyl dichloride (0.26 g) was similarly dissolved in 250 mL of dry dichloromethane and transferred to an identical dropping funnel. These two solutions were added dropwise to 1200 mL of dry dichloromethane over a period of 4 h with stirring under nitrogen. The reaction mixture was then stirred for a further 12 h. The precipitate was filtered off and the solvent evaporated under reduced pressure. The products were chromatographed on silica with chloroform–ethanol eluant. Fraction A was eluted with chloroform. Fraction B was eluted with chloroform–ethanol (99:1). Fraction C was eluted with chloroform–ethanol (98:2). All three fractions were recrystallized from chloroform–pentane.

Fraction A was obtained as a white crystalline solid (400 mg, 34%). The NMR data are discussed in the main text. *m/z* 1806 (MH^+); $C_{120}H_{128}N_8O_8$ requires M^+ = 1808.

Fraction B was obtained as a white powder (600 mg, 51%). Spectroscopic data were as for the cyclic dimer **1** from Scheme I.

Fraction C was obtained as a white powder (50 mg, 5%). NMR ($CDCl_3$/CD_3OD) δ 8.41 (4 H, s), 7.98 (8 H, d), 7.43 (4 H, t), 6.96 (16 H, s), 2.21 (16 H, br), 2.10 (48 H, s), 1.52 (24 H, br). *m/z* 1806 (MH^+); $C_{120}H_{128}N_8O_8$ requires M^+ = 1808.

Conclusion

The three-dimensional structure of a new [2]-catenane has been determined by using ^1H NMR spectroscopy. This structure agrees well with the predictions of molecular mechanics calculations except in the orientation of one of the amide groups, which has not been unambiguously determined. The catenane is locked into a well-defined conformation by several intermacrocycle H-bonds and π–π interactions. The dynamic properties of the system were investigated by using variable-temperature ^1H NMR. The inside and outside parts of the molecule cannot exchange with one another due to the bulky cyclohexyl groups, which act as spokes preventing free rotation of the macrocycles. The molecule does have some conformational mobility in that the inside isophthaloyl groups can pass through the macrocyclic cavities and this leads to a 90° rocking motion. The activation energy for this process is 73 kJ mol^{-1} and this large activation barrier means that the catenane adopts a chiral ground state. Splitting observed in the ^1H NMR spectrum in the presence of a chiral shift reagent provided experimental evidence of this chirality. The catenane switches between its two enantiomeric conformations at a rate of 1 s^{-1} at room temperature.

The intermacrocycle interactions inferred from the spectroscopic and modeling studies must play an important role in formation of the catenane. The macrocycle, **1**, was originally designed to complex *p*-benzoquinone using H-bonding and π–π interactions.[7] It is therefore not surprising that it should complex an isophthaloyl moiety via the same combination of interactions: the isophthaloyl unit is also π-electron deficient and has two carbonyl oxygens available for H-bonding. Thus H-bonding and π–π interactions must be responsible for templating the self-assembly of the interlocked ring system. This leads to a remarkably efficient supramolecular synthesis: the catenane was obtained in 34% yield in a one-pot double-macrocyclization reaction with no attempt made to optimize the yield. Moreover, the reaction was carried out under high-dilution conditions, which should inhibit self-association of the reactants.[17,18] In other words, the templating does not occur prior to reaction à la Sauvage[4,7b] but subsequent to formation of one or more of the amide bonds.[1] Further investigations into the sequence of events leading to catenane formation are in progress.

Acknowledgment. I thank Jane Clift and Dr. J. K. M. Sanders for helpful discussion and the referees for comments on an earlier version of this manuscript.

Registry No. 1, 135328-02-8; **2**, 141272-43-7; **4**, 22657-66-5; **5**, 141062-51-3; $ClCOC_6H_4$-*n*-COCl, 99-63-8; cyclohexanone, 108-94-1; 2,6-dimethylaniline, 87-62-7.

Supplementary Material Available: A table of all cross-peaks observed in the NOESY spectra of the catenane (1 page). Ordering information is given on any current masthead page.

(17) In ^1H NMR studies, the reactants showed no signs of self-association at 10^{-2} M concentrations in CD_2Cl_2. The maximum possible concentration of reactants in the high-dilution vessel was 8×10^{-4} M.

(18) Self-complexation and aggregation of related molecules in aqueous solution have been examined. (a) Diederich, F.; Dick, K. *Tetrahedron Lett.* **1982**, *32*, 3167–3170. (b) Diederich, F.; Dick, K. *J. Am. Chem. Soc.* **1984**, *106*, 8024–8036. (c) Diederich, F.; Dick, K.; Griebel, D. *Chem. Ber.* **1985**, *118*, 3588–3619. (d) Diederich, F. *Angew. Chem., Int. Ed. Engl.* **1988**, *27*, 362–386. (e) Murakami, Y. *Top. Curr. Chem.* **1983**, *115*, 107–155.